ARTICLES SCIENCE CHINA Materials

mater.scichina.com link.springer.com

Published online 7 March 2018 | https://doi.org/10.1007/s40843-018-9233-9
Sci China Mater 2018, 61(9): 1154–1158

Optical visualization of MoS_2 grain boundaries by gold deposition

Lulu Sun[1,2] and Jian Zheng[1*]

ABSTRACT **The grain boundaries (GBs) in continuous films or domains of MoS_2 are vital to its optical and electrical properties. Almost all previous approaches for GBs visualization are based on microscopy and spectroscopy and only effective for domains with less than several micrometers in size. Here we report a simple method for the visualization of large GBs in MoS_2 surface by optical microscope. Gold was deposited on the MoS_2 grown by chemical vapor deposition, and then the GBs could be observed by optical microscope. Upon gold deposition on MoS_2, the entire GBs of large-area MoS_2 were clearly visualized using this method. To verify the result, the GBs were also characterized *via* scanning electron microscopy, transmission electron microscopy and atomic force microscopy. It showed the small particles of gold were clustered together on GBs, which had a larger binding energy than the inner regions. The method is universal and allows for the nondestructive identification of the GBs in any two dimensional materials with large area.**

Keywords: grain boundaries, gold deposition, optical microscope, single layer MoS_2

INTRODUCTION

Single layer MoS_2 has attracted considerable interest for its potential application in novel electronic and optoelectronic devices [1–4]. High quality, large-area and single-layer MoS_2 can be fabricated by chemical vapor deposition (CVD) [5–6], but the grain boundary (GB) is inevitable and difficult to be identified. GBs affect the electron transfer process, and degrade the electrical and mechanical performances of MoS_2, which limit the application of MoS_2 [7–10]. In previous reports, GBs were studied using scanning tunneling microscopy (STM) [11], transmission electron microscopy (TEM) [12] and electron diffraction; hence several factors were inevitable, such as the requirement for complicated sample preparation, time delays, and a limited observation area. Therefore, it is urgent to find a simple and convenient method to study the GBs. As a previous report, GBs are observed by oxidation of copper substrate under optical microscopy [13–15], in which the substrate is required to be metal or be easily oxidized.

In this paper, we propose one feasible method to identify GBs directly by optical microscope on Si/SiO_2 substrate with depositing gold on MoS_2, which depends on the difference of diffusion coefficient of gold on the surface of MoS_2 between the GBs and the inner domains. This method offers unique advantages in the light of rapid imaging and the ability to identify GBs in large-area two dimensional (2D) materials without complicated sample preparation processes, which may arouse undesired artefacts, such as cracks and wrinkles. The results are confirmed by scanning electron microscopy (SEM), TEM, and atomic force microscopy (AFM). This method can be used to damage-freely identify any 2D materials with large size.

EXPERIMENTAL SECTION

Growth of monolayer MoS_2

The monolayer MoS_2 grew on Si with 300 nm of SiO_2, which was placed face-down above a ceramic boat containing MoO_3 powder (20 mg, 99.95%, Alfa Aesar) by CVD method. The ceramic boat was loaded in the heating zone center of the furnace tube, where another boat containing sulfur (80 mg, 99.999%, Alfa Aesar) was located upstream. The tube was first purged with ultrahigh-purity Ar for 30 min at a flow rate of 200 sccm. Then, the furnace was heated to 500°C within 12 min, 500°C to 720°C in another 20 min, and then kept at 720°C for 5 min. The sulfur was heated to 130°C with a separate heat belt as the furnace reached 720°C. During the

[1] State Key Laboratory of Organic Solids, the Institute of Chemistry, Chinese Academy of Sciences, Beijing 100190, China
[2] School of Materials Science and Engineering, Qingdao University of Science & Technology, Qingdao 266042, China
* Corresponding author (email: zhengjian@iccas.ac.cn)

growth, Ar as carrier gas was maintained at a flow rate of 10 sccm, and then the system was rapidly cooled down to room temperature.

Gold deposition and annealing

The as-prepared single layer MoS_2 was placed in a glovebox and gold (99.99%, Sigma-Aldrich) was deposited onto it with thermal evaporator under 5×10^{-4} Pa. The thickness of the gold was 30 nm, controlled by current. After deposition, the sample was annealed at 50, 75, 100°C respectively for 30 min under vacuum.

Characterization

Poly(methyl methacrylate) (PMMA) layer was spin-coated on the surface of $MoS_2/SiO_2/Si$ and annealed at 80°C for 30 min to improve the adhesion and eliminate air bubbles between MoS_2 and PMMA. Then the sample was placed into 2 mol L^{-1} KOH to etch the SiO_2 and then the PMMA/MoS_2 was detached from the substrate. The PMMA/MoS_2 film was then transferred onto a TEM grid and washed with deionized water and then dried under ambient. Finally, the PMMA layer was removed by heating at 300°C for 6 h. TEM images were obtained with JEOL JEM-2100F at an accelerating voltage of 200 kV. SEM (HITACHI S-4800) was used to examine the surface morphology of the samples at an accelerating voltage of 15 kV. AFM were taken on Multimode Nanoscope V with tapping mode. Raman spectrum was excited with 532 nm laser with HORIBA HR Evolution.

RESULTS AND DISCUSSION

Fig. 1a shows an optical micrograph of the typical triangular-shaped MoS_2 with size approximately 80 μm grown on Si/SiO_2 by CVD method. In photoluminescence (PL) spectrum and the fluorescence micrograph of MoS_2 (Fig. 1f), a strong peak at about 683 nm, corresponding to the 1.82 eV direct band gap reveals the formation of single layered crystalline MoS_2 [16–19]. TEM, high resolution TEM (HRTEM) and selected area electron diffraction (SAED), depicted in Fig. 1c, d, confirm that the MoS_2 is single layered and high crystallinity, with the six-fold symmetry diffraction spots and periodical lattice [20,21]. Raman spectrum displays two Raman characteristic peaks, the in-plane vibrational mode E_{2g}^1 (385 cm^{-1}) and out-of-plane vibrational mode A_{1g} (406 cm^{-1}), in Fig. 1e, and the gap between E_{2g}^1 and A_{1g} is 21 cm^{-1}, verifying that the as-synthesized MoS_2 is single layered [22,23]. When two or more triangle met together, the GBs formed, as shown in Fig. 1b.

Generally the GBs are in nano-size and can only be identified by microscopy and spectroscopy. To study the GBs in the single layered crystalline MoS_2, the gold was deposited on MoS_2 with 10 nm and 20 nm. Because the thinner film is not favorable for observing the GBs (Fig. S1), the gold was deposited 30 nm, controlled by current, using a thermal evaporator under 5×10^{-4} Pa at 100°C, and then annealed at 50, 75, 100°C for 30 min respectively (Fig. 2a–c). Fig. 2a shows optical image of MoS_2 sheet with gold deposited after annealed at 50°C. GBs do not appear. Fig. 2d shows that GBs are completely invisible under this condition with dark field optical microscopy. Fig. 2b shows the optical image of MoS_2 sheet with gold deposited after annealed at 75°C, where the GBs are discontinuous. Corresponding dark field optical image shows the GBs are not clear and discontinuous (Fig. 2e), and gold uniformly assembles on the MoS_2 sheet. After annealing at 100°C, gold clusters into lines along the GBs, which are visualized by optical microscopy and dark field optical microscopy, as respectively shown in Fig. 2c, f. GBs can be found by optical microscopy in the sample annealed at 100°C for 30 min and lower temperature annealing results in inconspicuous gold line and cannot define the GBs.

With the gold deposition, the steam at the surface of MoS_2, moves randomly, and forms nucleation points in the MoS_2 surface. As the annealing temperature gradually increases, the small gold particles increase and gradually form large particles. The schematic representation of GBs formation is given in Fig. 3a. The small gold nanoparticles are deposited onto the MoS_2 surface *via* thermal evaporation. Then upon annealing, the gold cluster into large

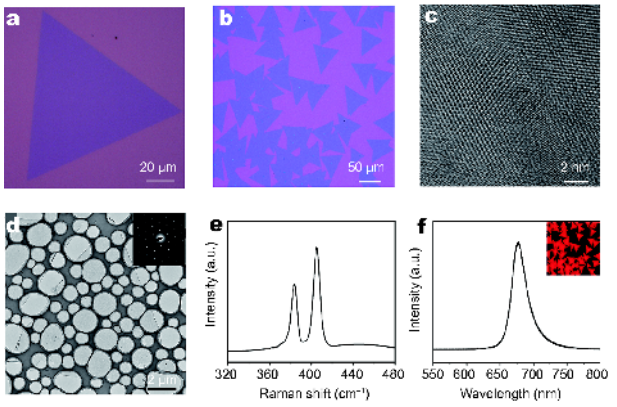

Figure 1 TEM and Raman characterization of CVD-grown monolayer MoS_2. (a, b) Optical images of the monolayer MoS_2. (c) High-resolution TEM image of MoS_2. (d) Low-resolution TEM image of the MoS_2 flakes and SAED image of the MoS_2 triangle. (e) Raman spectrum of a monolayer MoS_2 triangle. (f) PL spectrum of a monolayer MoS_2 triangle, inset: fluorescence image of triangular MoS_2 domains.

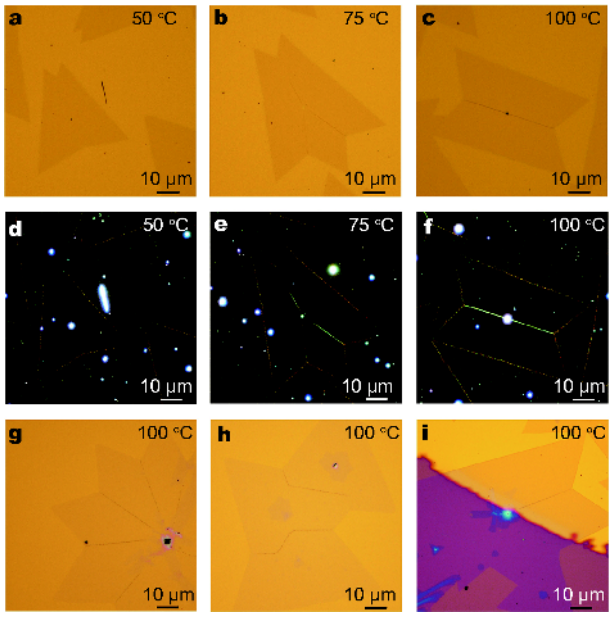

Figure 2 Optical images of the grain boundaries with deposited gold and annealing on the surface. (a) A monolayer of MoS_2 after gold deposition and annealing at 50°C for 30 min. (b) A monolayer of MoS_2 annealed at 75°C for 30 min, with discontinuous GBs. (c) A monolayer of MoS_2 after gold deposition and annealing at 100°C for 30 min, resulting in the appearance of GBs clearly. (d–f) Dark field optical microscopy images of MoS_2 corresponding to (a–c). (g) A monolayer of $MoSe_2$ GBs was observed under optical microscope after annealed at 100°C for 30 min. (h) A monolayer of WSe_2 with GBs after annealed at 100°C for 30 min. (i) A monolayer of WS_2 with grain boundaries after annealed at 100°C for 30 min.

particles with hundreds of nanometer size in the GBs, because the binding energy of GBs is higher than that of the basal plane according to first-principles calculation [24–28] where the gold are prior to cluster at the GBs. As shown in Fig. 3b–d, the SEM images verify that the gold almost evenly deposited on the MoS_2 surface, and the average size of gold nanoparticles on the GBs is larger than that in the basal plane. Upon annealing the gold cluster into particles with hundreds of nanometer size along the GBs, and this quasi-one-dimensional (1D) structure could be directly imaged by optical microscopy. In addition, we found that the gold particles are only clustered at the GBs. Therefore, the gold particles showed different appearances in the grain boundary and inside. The gold can easily accommodate near the GBs into the non-moving gold clusters, which attract other gold atoms or small gold clusters to grow, due to the defects and dangling bonds.

AFM images further identify the GBs. As shown in Fig. 4, the gold particles are approximately 0.48 μm in diameter, which is large enough to be detected by an optical

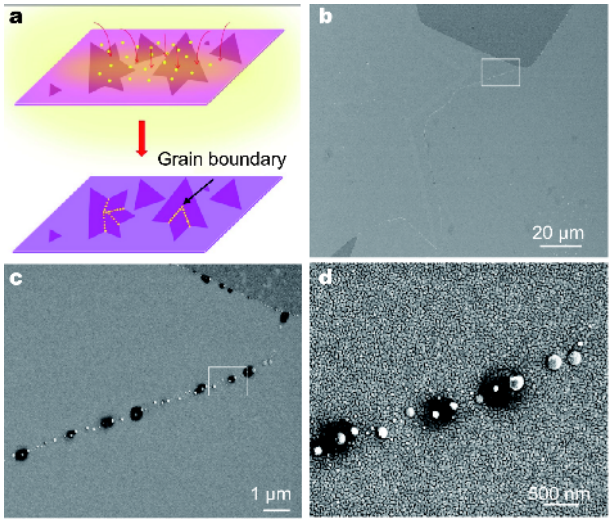

Figure 3 SEM images of grain boundaries after gold deposition and annealing. (a) The appearance process of grain boundaries. (b) Low-resolution SEM of GBs resulting in the appearance of lines. (c) High-resolution SEM of GBs shows gold particles presented in (b). (d) High-resolution SEM shows gold morphologies presented in (c).

microscope. During annealing, the small particles of gold move gradually and accumulate into large particles along the GBs, because gold tend to cluster together at the sites with larger binding energy. The inner regions of MoS_2 cannot provide higher energy, so the gold particles are relatively stable. The mobility of gold was retuned during annealing, and the different surface structures would be represented by the morphology of gold.

This method is also applied to define the GBs of other 2D materials, such as $MoSe_2$, WSe_2 and WS_2. As shown in Fig. 2g–i, the GBs of $MoSe_2$, WSe_2 and WS_2 can be easily imaged by optical microscope. We also compare the morphology of one sample with and without gold deposition, as shown in Fig. 2i, the left part and right part corresponding to the as-prepared single crystalline WS_2 and the part with gold film, respectively. It is clear that the GBs could be directly located. Therefore, this approach is universal to nondestructively determine the GBs of various 2D materials without ever needing to consider the complicated sample preparation.

CONCLUSION

The GBs on the single layered crystalline MoS_2 could be directly imaged under optical microscope by gold deposition with nondestruction. The optimized condition of gold deposition was 100°C and annealing at this temperature for 30 min. Because of the different binding energy on the GBs and inner area, the gold crumped along the GBs and was large enough to be seen by optical

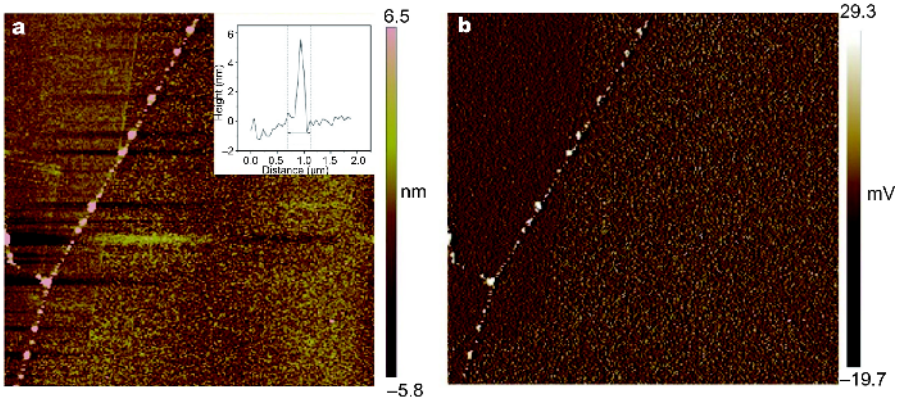

Figure 4 Topological characterizations of the GBs using AFM. (a) AFM topological mapping of the MoS_2 GBs and as-obtained topological line profile. (b) Close-up mapping of MoS_2 GBs.

microscope. SEM and AFM, evidencing the optical microscope results, can also locate the GBs. This method can also be applied to other 2D materials with large size.

Received 3 January 2018; accepted 13 February 2018; published online 7 March 2018

1 Fiori G, Bonaccorso F, Iannaccone G, *et al.* Electronics based on two-dimensional materials. Nat Nanotechnol, 2014, 9: 768–779
2 Liu J, Cao H, Jiang B, *et al.* Newborn 2D materials for flexible energy conversion and storage. Sci China Mater, 2016, 59: 459–474
3 Cui J, Xu S, Wang L. Monolayer MoS_2 decorated Cu_7S_4-Au nanocatalysts for sensitive and selective detection of mercury(II). Sci China Mater, 2017, 60: 352–360
4 Kim IS, Sangwan VK, Jariwala D, *et al.* Influence of stoichiometry on the optical and electrical properties of chemical vapor deposition derived MoS_2. ACS Nano, 2014, 8: 10551–10558
5 Wu Y, Wang D, Li Y. Understanding of the major reactions in solution synthesis of functional nanomaterials. Sci China Mater, 2016, 59: 938–996
6 Yang X, Li Q, Hu G, *et al.* Controlled synthesis of high-quality crystals of monolayer MoS_2 for nanoelectronic device application. Sci China Mater, 2016, 59: 182–190
7 Meng R, Jiang J, Liang Q, *et al.* Design of graphene-like gallium nitride and WS_2/WSe_2 nanocomposites for photocatalyst applications. Sci China Mater, 2016, 59: 1027–1036
8 Lehockey EM, Brennenstuhl AM, Thompson I. On the relationship between grain boundary connectivity, coincident site lattice boundaries, and intergranular stress corrosion cracking. Corrosion Sci, 2004, 46: 2383–2404
9 Zheng W, Feng W, Zhang X, *et al.* Anisotropic growth of non-layered CdS on MoS_2 monolayer for functional vertical heterostructures. Adv Funct Mater, 2016, 26: 2648–2654
10 Feng W, Zheng W, Cao W, *et al.* Back gated multilayer InSe transistors with enhanced carrier mobilities *via* the suppression of carrier scattering from a dielectric interface. Adv Mater, 2014, 26: 6587–6593
11 Koepke JC, Wood JD, Estrada D, *et al.* Atomic-scale evidence for potential barriers and strong carrier scattering at graphene grain boundaries: a scanning tunneling microscopy study. ACS Nano, 2013, 7: 75–86
12 Huang PY, Ruiz-Vargas CS, van der Zande AM, *et al.* Grains and grain boundaries in single-layer graphene atomic patchwork quilts. Nature, 2011, 469: 389–392
13 Duong DL, Han GH, Lee SM, *et al.* Probing graphene grain boundaries with optical microscopy. Nature, 2012, 490: 235–239
14 Yu SU, Cho Y, Park B, *et al.* Fast benchtop visualization of graphene grain boundaries using adhesive properties of defects. Chem Commun, 2013, 49: 5474–5476
15 Cassereau L, DuFort CC, Weaver VM. Laying down the tracks. Nat Mater, 2012, 11: 490–492
16 Radisavljevic B, Radenovic A, Brivio J, *et al.* Single-layer MoS_2 transistors. Nat Nanotechnol, 2011, 6: 147–150
17 Schmidt H, Wang S, Chu L, *et al.* Transport properties of monolayer MoS_2 grown by chemical vapor deposition. Nano Lett, 2014, 14: 1909–1913
18 Zhang J, Yu H, Chen W, *et al.* Scalable growth of high-quality polycrystalline MoS_2 monolayers on SiO_2 with tunable grain sizes. ACS Nano, 2014, 8: 6024–6030
19 Lee YH, Zhang XQ, Zhang W, *et al.* Synthesis of large-area MoS_2 atomic layers with chemical vapor deposition. Adv Mater, 2012, 24: 2320–2325
20 Jeon J, Jang SK, Jeon SM, *et al.* Layer-controlled CVD growth of large-area two-dimensional MoS_2 films. Nanoscale, 2015, 7: 1688–1695
21 Yin Z, Li H, Li H, *et al.* Single-layer MoS_2 phototransistors. ACS Nano, 2012, 6: 74–80
22 Li H, Zhang Q, Yap CCR, *et al.* From bulk to monolayer MoS_2: evolution of raman scattering. Adv Funct Mater, 2012, 22: 1385–1390
23 Windom BC, Sawyer WG, Hahn DW. A Raman spectroscopic study of MoS_2 and MoO_3: applications to tribological systems. Tribol Lett, 2011, 42: 301–310
24 Holm EA, Olmsted DL, Foiles SM. Comparing grain boundary energies in face-centered cubic metals: Al, Au, Cu and Ni. Scripta Mater, 2010, 63: 905–908
25 Alexander KC, Schuh CA. Exploring grain boundary energy landscapes with the activation-relaxation technique. Scripta Mater, 2013, 68: 937–940
26 Uesugi T, Higashi K. First-principles calculation of grain boundary energy and grain boundary excess free volume in aluminum: role of grain boundary elastic energy. J Mater Sci, 2011, 46: 4199–4205

27 Zou X, Liu Y, Yakobson BI. Predicting dislocations and grain boundaries in two-dimensional metal-disulfides from the first principles. Nano Lett, 2012, 13: 253–258
28 Gunlycke D, Vasudevan S, White CT. Confinement, transport gap, and valley polarization in graphene from two parallel decorated line defects. Nano Lett, 2013, 13: 259–263

Acknowledgements This work was supported by the Strategic Priority Research Program of the Chinese Academy of Sciences (XDB12010000), and the National Natural Science Foundation of China (21573253).

Author contributions Zheng J designed the project and Sun L synthesized and characterized the materials.

Conflict of interest The authors declare no conflict of interest.

Supplementary information Supporting data are available in the online version of the paper.

Lulu Sun is now a master candidate at the School of Materials Science and Engineering, Qingdao University of Science & Technology. She is jointly supervised by Prof. Jian Zheng at the Institute of Chemistry, Chinese Academy of Sciences. Her research focuses on the synthesis and characterization of 2D materials.

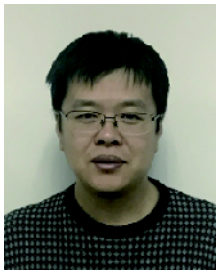

Jian Zheng received his PhD degree in 2011 from the Institute of Chemistry, Chinese Academy of Sciences. Then he worked as a Postdoc at National University of Singapore (2011–2015). Now he is a professor at the Institute of Chemistry Chinese Academy of Sciences. His current researches focus on the growth and characterization of 2D materials, and their applications in nano-electronics.

金沉积法使MoS_2晶界光学可视化

孙璐璐[1,2], 郑健[1*]

摘要 近年来, 二硫化钼因其独特的光学和电学性能引起了人们的广泛关注. CVD法生长的MoS_2上不可避免的存在很多晶界, 对其电学及光电性能具有很大影响. 以往观察晶界多采用电子显微镜和光谱, 且只能对几微米范围进行观察. 本文介绍了一种简单的沉积金的方法, 使MoS_2表面的晶界在光学显微镜下可见. 与晶面内相比晶界处具有更高的结合能, 更有利于金颗粒的聚集, 沉积后退火使得金颗粒进一步变大, 足以在光学显微镜下可见. 用这种方法大面积MoS_2晶界的始末端皆可以清楚地观察到. SEM, TEM, AFM的研究结果证实了以上方法的准确性. 该方法可用于任何大面积二维材料晶界的表征, 具有很强的普适性.

